

- One-pot, low-cost and reproducible g-C₃N₄ grafting onto silica microparticles
- g-C₃N₄@silica novel application for SPE of Fluoroquinolones from natural water
- Quantitative recovery in tap and raw river waters (low ng L⁻¹)
- Good precision and sensitivity for g-C₃N₄@silica SPE coupled to HPLC-FD
- g-C₃N₄@silica advantageous in terms of preparation, cost, efficiency, reusability

1 **Facile and fast preparation of low-cost silica-supported g-C₃N₄ for solid-phase** 2 **extraction of fluoroquinolone drugs from environmental waters**

3 Andrea Speltini,^{a*} Federica Maraschi,^a Roberta Govoni,^a Chiara Milanese,^a Antonella Profumo,^a
4 Lorenzo Malavasi^b, Michela Sturini^a

5
6 ^a*Department of Chemistry, University of Pavia, via Taramelli 12, 27100 Pavia, Italy*

7 ^b*Department of Chemistry, University of Pavia, and INSTM, via Taramelli 12, 27100 Pavia, Italy*

8 ^{*}*E-mail: andrea.speltini@unipv.it; Fax: +39 0382-528544; Tel.: +39 0382-987349*

9 10 **Abstract**

11 The analytical application of silica-supported graphitic carbon nitride (g-C₃N₄) for solid-phase extraction
12 (SPE) of fluoroquinolone (FQ) pollutants from water is presented for the first time. g-C₃N₄ was easily and
13 quickly prepared by one-pot thermal condensation of dicyandiamide and characterized by powder X-ray
14 diffraction, thermogravimetric analysis, scanning electron microscopy, Fourier transform infrared
15 spectroscopy and surface area measurements. The novel composite was applied as sorbent for SPE of FQs
16 from water prior high-performance liquid chromatography with fluorescence detection. The extraction
17 efficiency of g-C₃N₄ was tested in tap and surface waters at actual concentrations (10-100 ng L⁻¹).
18 Quantitative adsorption was achieved using 100 mg sorbent (20 wt% g-C₃N₄) for pre-concentration of 50-
19 500 mL sample, at the native pH (~ 7.5-8). Elution was performed with 25 mM H₃PO₄ aqueous solution-
20 acetonitrile (80:20), obtaining recoveries in the range 70-101%, enrichment factors up to 500 and inter-day
21 RSDs ≤ 12 %. The batch-to-batch reproducibility was assessed on 3 independently synthesized g-
22 C₃N₄@silica preparations (RSD < 6-12 %). g-C₃N₄ supported on silica microparticles proved to be of easy
23 preparation, costless, reusable for at least 4 extractions of raw surface waters and suitable for determination
24 in real matrices.

25
26 **Keywords:** Antibiotics; Determination; Graphitic carbon nitride; Pollutants; Sample preparation; Sample
27 enrichment

29 1. Introduction

30 Graphitic carbon nitride (g-C₃N₄), the most stable allotrope of carbon nitride mainly made of carbon and
31 nitrogen, is presently considered the most promising candidate to complement carbon materials. g-C₃N₄ is
32 the newest carbon-based 2D material and shows a “graphene-like” structure of layered sheets of tri-s-triazine
33 connected via tertiary amines. These form a defected-rich and N-bridged macromolecular structure that can
34 be easily swelled and exfoliated by aqueous sonication into nearly transparent ultrathin nanosheets, stable in
35 both acidic and alkaline media [1]. The synthesis, entailing use of simple precursors under ambient
36 conditions [2,3], is easy and inexpensive and, for instance, can be carried out by thermally induced bulk
37 condensation or pyrolysis of melamine or urea [4-9], also with no need for additives such organic solvents
38 [8].

39 In the last years, g-C₃N₄ proved to have great potentiality in many fields, including sensing [10], bioimaging
40 [11] and photocatalysis [12,13], and in principle could be a very efficient sorbent in analytical sample
41 preparation. Because of its similarity to graphene, good compatibility with aqueous phase and expected great
42 affinity for a wide range of compounds, g-C₃N₄ is a very promising sorbent for solid-phase extraction (SPE)
43 [14,15]. Indeed, its double-sided polyaromatic scaffold shows both sides of the planar sheets available for
44 molecules adsorption, and the large π -electron system also endows a strong affinity for carbon-based ring
45 structures, typical of many drugs, pollutants, and biomolecules [5].

46 Few papers are currently available on the application of g-C₃N₄ for pre-concentration purposes, specifically
47 in batch (magnetic) extraction [5-8,16,17] and solid-phase microextraction (SPME) [4], but none of them
48 deals with application to column-SPE. Nonetheless, the use of g-C₃N₄ for SPE of pharmaceuticals,
49 fluoroquinolones (FQ) included, from water is not documented at present.

50 FQs, antibiotics for human and veterinary medicine endowed with broad activity spectrum and good oral
51 absorption, are an important class of emerging contaminants. Their occurrence, assessed in various
52 environmental compartments [18,19], is essentially due to the partial metabolization and partial abatement by
53 wastewater treatment plants (WWTPs) [20]. This causes the release of pharmaceutically active drugs into
54 water basins, affecting their transformation/removal rates. Moreover, the common practice of recycling
55 manure from livestock farming and sewage sludge from WWTPs as fertilizers, and recycling of sludge for

56 the production of compost, widely employed as soil conditioner/fertilizer, are other major contamination
57 routes [21,22]. Despite FQs photosensitivity, both in water [23,24] and soil systems [25] their presence in the
58 environment implicates serious threats to the ecosystem and humans. Mainly, toxicity [24], bacterial
59 resistance stimulation [26] and formation of pharmacologically active photoproducts that contribute to the
60 overall impact [24,27]. It is evident that monitoring FQs in the environment is a priority task that needs
61 accurate, robust and sensitive analytical methods. In particular, the low concentrations detected in surface
62 waters (typically tens ng L⁻¹) require a SPE pre-concentration step prior instrumental analysis [28-32]. SPE
63 can be carried out by reversed-phase or mixed-mode polymer-based sorbents [33]. Recently, graphene – a
64 2D carbon material capable of multi-type interaction – grafted onto silica microparticles, has been proposed
65 for FQs pre-concentration [34].

66 Prompted by the performance of mixed-mode sorbents, herein we report the preparation and characterization
67 of a composite consisting of silica-supported g-C₃N₄, and its original application as SPE sorbent. g-C₃N₄ was
68 grafted onto silica in order to have a sorbent to be easily used in conventional SPE columns, thus avoiding
69 the excessive packaging that would otherwise occur using the bulk material [7]. The preparation of the
70 material, simple and costless, is carried out by mixing the g-C₃N₄ precursor (in the present case
71 dicyandiamide) and silica followed by a thermal treatment under nitrogen environment. g-C₃N₄@silica has
72 been characterized by X-ray diffraction (XRD), thermogravimetric analysis (TGA), scanning electron
73 microscopy (SEM), Fourier transform infrared spectroscopy (FTIR) and surface area measurements (BET),
74 and tested as SPE sorbent for pre-concentration of Ciprofloxacin (CIP), Danofloxacin (DAN), Enrofloxacin
75 (ENR), Levofloxacin (LEV) and Marbofloxacin (MAR) from environmental waters. After SPE on g-
76 C₃N₄@silica, separation and quantification were performed by high performance liquid chromatography
77 coupled with fluorescence detection (HPLC-FD).

78

79 **2. Experimental**

80 **2.1 Chemicals and materials**

81 All chemicals were reagent grade or higher in quality. Silica (< 63 µm/230 mesh) from Merck (Darmstadt,
82 Germany) was used. Analytical grade FQs standards (CIP, DAN, ENR, LEV, MAR), tetrabutylammonium
83 hydroxide (TBAH, 1 M in H₂O), ethanol (≥ 99.8 %), dicyandiamide (99 %), polypropylene tubes and

84 polyethylene frits were supplied by Sigma-Aldrich (Milan, Italy). HPLC gradient grade acetonitrile (ACN)
85 and methanol (MeOH) were purchased by VWR (Milan, Italy). H₃PO₄ (85 %, w/w), HCl (37 %, w/w), NH₃
86 (30 %, w/w) and anhydrous NaOH (97 %) were obtained from Carlo Erba Reagents (Milan, Italy). Ultrapure
87 water (resistivity 18.2 MΩ cm⁻¹ at 25 °C) was produced by a Millipore Milli-Q system. pH was measured by
88 an Orion 420A pH meter (Thermo Electron, Rodano, Italy). FQs stock solutions of 200 μg mL⁻¹ were
89 prepared in MeOH containing 0.1 % (v/v) 1 M NaOH and stored in the dark (4 °C). FQs working solutions
90 of 600 μg L⁻¹ in 25 mM H₃PO₄ aqueous solution were renewed weekly. Laboratory operations were
91 conducted under red light.

92

93 **2.2 Synthesis of g-C₃N₄@silica**

94 Dicyandiamide was dissolved in ethanol-water (4:1) by heating to 80 °C and kept at this temperature for 5
95 min to ensure all the reagent was dissolved. To this solution, proper amounts of silica to obtain 5, 20 and 50
96 wt% g-C₃N₄@silica composites, were added and the mixture stirred vigorously. After that, the mixture was
97 heated at 100 °C until the ethanol and water were evaporated and a white solid was obtained. The resulting
98 material was then dried at 100 °C in an air oven overnight and thermally treated in N₂ atmosphere at 550 °C
99 for 4 h with a heating ramp of 1 °C min⁻¹ and a cooling ramp of 10 °C min⁻¹ [35].

100

101 **2.3 Characterization of g-C₃N₄@silica**

102 XRD patterns have been collected on a Bruker D8 Advance diffractometer using a Cu Kα radiation between
103 5 and 35° with step size 0.02°. TGA has been carried out with a Q5000 thermobalance (TA Instrument)
104 under N₂ atmosphere between room temperature and 750 °C. Microstructural characterization of the samples
105 was made using a high-resolution scanning electron microscope (SEM, TES- CAN Mira 3) operated at 15
106 kV. FTIR spectra were recorded using a Nicolet FT-IR iS10 spectrometer (Nicolet, Madison, WI) equipped
107 with ATR (attenuated total reflectance) sampling accessory (Smart iTR with ZnSe plate) by coadding 256
108 scans in the 4000-650 cm⁻¹ range at 4 cm⁻¹ resolution. Specific surface area measurements were performed
109 by a Sorptomatic 1990 instrument by Thermo Fisher Scientific. About 350 mg of powder was charged in the
110 glass sample holder and degassed at 100 °C for 60 h. Subsequently, samples were cooled down at -196 °C

111 and 2 adsorption–desorption cycles followed by a last adsorption run were performed (BET method,
112 analyzing gas N₂, 50 points for run; blank done in He before the first adsorption run).

113

114 **2.4 Water samples**

115 Tap water was from the Pavia municipal waterworks. Northern Italy surface waters were collected at 30-50
116 cm depth, directly in amber glass bottles, from Ticino River, Adda River, Naviglio Pavese River, Garda Lake
117 and from a ditch downstream swine farms near Pavia (physical-chemical parameters reported in
118 Supplementary Data). Samples were stored in the dark (4 °C) and analyzed within 24 h.

119

120 **2.5 g-C₃N₄@silica SPE procedure**

121 The cartridges (6 mL polypropylene tubes, 12 mm inner diameter, 65 mm length) were prepared by placing
122 100 mg g-C₃N₄@silica between two polyethylene frits, and were washed under vacuum with 30 mL MeOH
123 followed by 50 mL ultrapure water to remove impurities and minimize void/channeling effect. For the
124 extraction procedure, performed by means of a vacuum system (Resprep manifold, Restek Corporation,
125 Bellefonte, USA), the cartridge was conditioned with 5 mL MeOH and 5 mL ultrapure water; the water
126 sample (50-500 mL) was fed to the column at a flow rate of ca. 2 mL min⁻¹, and then the cartridge was dried
127 under vacuum for 5 min. The analytes were simultaneously eluted (1 mL min⁻¹) with 6 mL 25 mM H₃PO₄
128 aqueous solution-ACN (80:20) and submitted to HPLC-FD analysis. For sample concentrations lower than
129 50 ng L⁻¹, the extracts were evaporated to 1 mL by XpressVapTM microwave accessory (radiation power 800
130 W, 13 min, CEM MarsXpress). For reusability tests, the cartridge was washed with 20 mL extracting
131 solution to avoid potential carry over.

132

133 **2.6 Liquid chromatography with fluorescence detection**

134 The HPLC-FD system consisted of a pump Series 200 equipped with vacuum degasser and interfaced with a
135 programmable fluorescence detector (Perkin Elmer, Monza, Italy). A Thermo Scientific AccucoreTM Polar
136 Advantage II C18 column (4.6 × 150 mm, 3 μm, 120 Å), purchased from Microcolumn (Lissone, Italy), was
137 used coupled to a similar guard-column. After 5 min equilibration, 50 μL of each sample was injected into
138 the HPLC system. The FD excitation/emission wavelengths selected were 280/450 nm for CIP, DAN and

139 ENR, 280/500 nm for LEV, and 297/507 nm for MAR. Elution was performed in 25 mM H₃PO₄-ACN
140 (87:13) for 6 min, followed by a 1 min linear gradient to 25 mM H₃PO₄-ACN (90:10), then isocratic elution
141 for 18 min (1 mL min⁻¹).
142

143 **2.7 Analytical evaluation**

144 Since the aim was applying g-C₃N₄@silica for pre-concentration of FQs from real samples, the whole
145 analytical procedure was evaluated. In the absence of certified reference materials (CRMs), trueness was
146 evaluated by recovery tests [36,37] in tap and river waters fortified in the range 10-100 ng L⁻¹ of each FQ.
147 The background FQs concentrations were checked by an independent method [34]. The inter-day precision
148 (within-laboratory reproducibility) was explicated as relative standard deviation (RSD%). Selectivity of
149 detection was checked from the HPLC-FD chromatograms of the SPE extracts obtained by pre-concentration
150 of raw river water [34,38] showing a negligible FQ native content (experimentally verified according to ref.
151 [34]). To calculate recovery at the concentrations expected after SPE, three independent calibration curves
152 (1-50 µg L⁻¹) were generated for each analyte in the SPE eluting solution, i.e. 25 mM H₃PO₄ aqueous
153 solution-ACN (80:20), as previously reported [39]. Method detection and quantification limits (MDL, MQL)
154 were experimentally determined. MDL was the minimum concentration that provided a FD signal
155 significantly different from zero, and MQL was the lowest concentration that provided acceptable recovery
156 (≥ 70 %) and precision (RSD < 20 %) [38]. The batch-to-batch reproducibility was assessed by recovery
157 tests on tap water spiked with 1 µg L⁻¹ of each drug, using 3 g-C₃N₄@silica powders independently
158 synthesized.
159

160 **3. Results and discussion**

161 **3.1 Characterization of g-C₃N₄@silica**

162 As reported in the Experimental part, three different composites have been synthesised, namely with 5, 20
163 and 50 wt% of g-C₃N₄. However, as highlighted later in the text, after a preliminary evaluation, the SPE
164 study has been carried out on the 20 wt% composite only, and for this reason we are reporting here the
165 characterization limited to this composition.

166 Fig. 1a shows the XRD patterns of pure silica, pure g-C₃N₄ and the g-C₃N₄@silica composite (20 wt% in g-
167 C₃N₄). As can be seen, silica is fully amorphous while g-C₃N₄ presents the common XRD pattern
168 characterized by two intense peaks around 12.8°, due to the intralayer distances, and around 27.5° related to
169 the distances between graphitic layers. The g-C₃N₄@silica composite presents an XRD pattern characteristic
170 of an amorphous sample as well. However, the absence of the features related to g-C₃N₄ is not due to the
171 formation of amorphous carbon nitride but to the relatively low amount of this phase (which is a bad
172 scatterer) in the composite. As a matter of fact, by increasing the amount of g-C₃N₄ in the composites it is
173 possible to observe the contribution to the XRD pattern of the graphitic phase as well (see for example the 50
174 wt% g-C₃N₄@silica composite in the Supplementary Data).

175 Thermogravimetry has been used to assess the actual amount of g-C₃N₄ present in the composite. As can be
176 inferred from Fig. 1b, above ca. 700 °C g-C₃N₄ is completely decomposed (see the green curve) while SiO₂
177 is stable up to that temperature. The weight loss for the g-C₃N₄@silica sample is around 17 % thus indicating
178 the successful loading of g-C₃N₄ on silica which is also close to the nominal value of 20 %. For this reason,
179 throughout this paper we are going to keep the nominal stoichiometry as reference by using, however, for the
180 discussion the real value determined by TGA.

181 Representative SEM images of the g-C₃N₄@silica 20 wt% composite are reported in Fig. 2. For comparison,
182 the SEM data for pure SiO₂ are as well shown. Pure silica is made of micron-size particles with flat and clean
183 surfaces, while the incorporation of g-C₃N₄ leads to the appearance of layered structures on the SiO₂ particles
184 surface.

185 FTIR measurements have been further used to confirm the successful loading of g-C₃N₄ on silica. Fig. 3
186 shows the spectra for pure silica, pure g-C₃N₄ and the g-C₃N₄@silica composite (20 wt% in g-C₃N₄). The
187 FTIR for pure g-C₃N₄ is in fully agreement with previous reported data on samples prepared starting from
188 dicyandiamide [40] and characterized by a sharp peak around 800 cm⁻¹ assigned to out-of-plane bending of
189 six-membered rings common to either triazine or eptazine structures [41]. Bands in the 1200-1600 cm⁻¹ range
190 are instead typical of C-N stretching and bending vibrations of nitrogen heterocycles. The FTIR spectrum of
191 amorphous silica (black line in Fig. 3) shows an intense peak around 1100 cm⁻¹ assigned to the Si-O-Si
192 asymmetric stretching vibration, while the peak at about 850 cm⁻¹ is characteristic of the Si-OH bending
193 from silica itself [42]. No hydroxyl groups are detected on the sample (expected to be present around 3500

194 cm^{-1}). The spectrum of $\text{g-C}_3\text{N}_4@\text{silica}$ (blue line in Fig. 3) presents characteristics feature of both pure silica
195 and $\text{g-C}_3\text{N}_4$. In particular, the $\text{g-C}_3\text{N}_4$ representative peaks are clearly visible in the 1200-1600 cm^{-1} region
196 (highlighted with a red ellipse) while the sharp peak around 800 cm^{-1} is superimposed to the Si-OH bending
197 peak of pure silica.

198 Finally, the surface area of the $\text{g-C}_3\text{N}_4@\text{silica}$ 20 wt% composite has been measured by means of gas
199 porosimetry method and resulted to be $210 \pm 5 \text{ m}^2 \text{ g}^{-1}$, to be compared to those of pristine silica ($450 \pm 5 \text{ m}^2$
200 g^{-1}) and pure $\text{g-C}_3\text{N}_4$ ($4 \pm 2 \text{ m}^2 \text{ g}^{-1}$).

201

202 **3.2 Solid-phase extraction on $\text{g-C}_3\text{N}_4@\text{silica}$**

203 Due to its aromatic nitrogen-rich 2D carbon structure, $\text{g-C}_3\text{N}_4$ is endowed with good polarity, water
204 compatibility and potential affinity for a wide range of molecules. Thus, it has great potentiality to be used as
205 mixed-mode sorbent for extraction of polar organics from water samples [14,15]. This is the case of FQs,
206 amphoteric compounds consisting of an aromatic quinolone core bearing polar ionisable groups, that in
207 principle are prone to interact with the $\text{g-C}_3\text{N}_4$ layers grafted onto silica.

208 The feasibility of using $\text{g-C}_3\text{N}_4@\text{silica}$ for SPE of FQs was first investigated in tap water, considering the
209 effect of various parameters, i.e. $\text{g-C}_3\text{N}_4$ silica loading, sorbent amount, sample volume and type/volume of
210 eluting solvent. Experiments in tap water samples – 50 mL, native pH, $5 \mu\text{g L}^{-1}$ MAR and ENR, 200 mg
211 sorbent, elution with $3 \times 5 \text{ mL } 10^{-3} \text{ M HCl}$ aqueous solution-ACN (80:20) – were initially undertaken to
212 investigate the affinity of FQ species for the material. The $\text{g-C}_3\text{N}_4$ loading (nominal 5-20-50 wt%) affected
213 both adsorption and desorption. Specifically, at the highest loading considerable amounts of FQs were not
214 retained (11-42 %), and 61-82 % of the sorbed fraction was eluted. At the lowest loading, despite better
215 adsorption (2-11 % not retained), elution was lower (58-64 %). This behaviour can be explained in terms of
216 $\text{g-C}_3\text{N}_4$ sheets aggregation, which is reasonably caused by increasing the loading. Accordingly, more active
217 sites available for adsorption should be present in $\text{g-C}_3\text{N}_4@\text{silica}$ 5 wt%, resulting in a stronger retention
218 capability. It was observed that the intermediate amount of $\text{g-C}_3\text{N}_4$ (i.e. 20 wt%) provided quantitative
219 removal of FQs from water (residual drugs < IDL) and mean recovery around 78 % (RSD < 14 %, $n=3$).
220 Elution was improved using 25 mM H_3PO_4 aqueous solution-ACN (80:20), requiring only 10 mL to elute the
221 analytes.

222 Since quantitative FQ adsorption from the sample was gained at the native pH, no pH adjustment was done.
223 This indicates good affinity of the analytes zwitterionic (globally uncharged) form for carbon nitride, clearly
224 due to the combination of Van der Waals, π stacking, dipole-dipole, hydrophobic and hydrogen bond
225 interactions [15]. This behaviour was in line with other mixed-mode phases [28,34]. Moreover, considering
226 that carbon nitride isoelectric point is around 4.5-5 [15,43] and that no significant variation in the recovery
227 was observed also in high-salinity samples (5-15 % w/v NaCl), π stacking seems to be the driving force for
228 FQ molecular adsorption.

229 Additional work was addressed to further investigate the elution step. Considering both the g-C₃N₄
230 isoelectric point and the zwitterionic nature of FQs (CIP pK_{a1} 5.90, pK_{a2} 8.89; DAN pK_{a1} 6.07-6.32, pK_{a2}
231 8.56-8.73; ENR pK_{a1} 6.27, pK_{a2} 8.3; LEV pK_{a1} 5.70-6.05, pK_{a2} 7.90-8.22; MAR pK_{a1} 5.51-5.69, pK_{a2}
232 8.02-8.58) [33] both acidic and alkaline solutions were tested. Fig. 4a gathers the responses obtained by SPE
233 of 250 mL tap water (100 ng L⁻¹ FQs) as function of the type of eluting phase.

234 The best elution was provided by 25 mM H₃PO₄ aqueous solution-ACN (80:20), successfully used also for
235 the commercial mixed-mode hydrophilic-lipophilic HLB polymer [44]. Inferior or higher ACN percentages
236 gave poorer recovery (data not shown). Lower recoveries were observed under alkaline conditions, i.e. 4 %
237 NH₃-MeOH (85:15), suggested for FQs elution using a variety of commercial cartridges [33]. Moreover,
238 differently from graphene [34], FQs were better desorbed in acidic solution rather than in 25mM TBAH
239 aqueous solution-ACN (70:30), hence use of ion pairing agents was not necessary. These findings could be
240 explained by the different polarity of the two 2D materials, and suggest that FQs desorption from g-C₃N₄ is
241 easier. This is justified by the lower aromaticity of g-C₃N₄ compared to graphene, involved by the C-N polar
242 bonds that decrease π -delocalization [15].

243 The effects of sorbent amount and elution volume are shown in Fig. 4b and 4c, respectively. These indicate
244 that FQs recovery is lowered in going from 100 to 300 mg g-C₃N₄@silica, and that volumes below 6 mL
245 were not convenient. Conversely, using higher sorbent amounts would require higher elution volumes, thus
246 lowering enrichment factor.

247 Under best conditions, i.e. 100 mg sorbent and 6 mL 25 mM H₃PO₄ aqueous solution-ACN (80:20) elution,
248 recovery in the range 70-101 % was obtained for the five drugs (Table 1). A typical chromatogram is
249 reported in Fig. 5.

250 The procedure has been tested also in raw river water, obtaining good extraction efficiency. The mean
251 recoveries, shown in Table 1, indicated that FQs adsorption is not hampered by other matrix constituents. As
252 displayed in Fig. 6, FD allowed selective detection of FQs in raw surface water, as no interfering signals
253 were noticed in “blank” river water (i.e. with negligible FQ native content) at the retention times of the 5
254 compounds.

255 It was found that 100 mg g-C₃N₄@silica 20 wt% (\equiv 20 mg g-C₃N₄) allowed SPE of 500 mL raw river water
256 spiked with FQs at 10-100 ng L⁻¹; moreover, clean extracts were obtained from actual matrices (see Fig. 6),
257 with no need for additional anion-exchange sample cleanup, that instead is necessary for FQs pre-
258 concentration using HLB SPE [44-46].

259 The cartridge proved to be reusable for more than one SPE, as that the extraction efficiency was maintained
260 also in raw river water for at least 4 runs (recovery > 70 %), accounting for good chemical/mechanical
261 stability of the composite.

262 The batch-to-batch reproducibility was assessed by recovery tests (100 mL tap water, 1 μ g L⁻¹ FQs) on 3
263 independent preparations of g-C₃N₄@silica. RSD values in the range 6-12 % accounted for good overall
264 reproducibility, from synthesis to instrumental analysis.

265 266 **3.3 Analytical performance of g-C₃N₄@silica SPE coupled to HPLC-FD**

267 The key features of the whole analytical procedure are hereafter summarized. The mean recoveries (%)
268 obtained in water samples spiked at environmentally significant concentrations are reported in Table 1.
269 Recovery was calculated as the ratio between the concentration determined in the g-C₃N₄@silica extract and
270 that expected after pre-concentration (calculated considering the initial amount of analyte and the enrichment
271 factor). As apparent, recovery was generally between 70 % and 101 % in tap water; quantitative extraction
272 (70-101 %) was also obtained in untreated river water spiked with 20-100 ng L⁻¹, and for ENR, LEV and
273 MAR recovery was good also at 10 ng L⁻¹ spike. Precision was evaluated by calculating the RSDs associated
274 to the mean recovery obtained for each concentration. As shown in Table 1, the inter-day precision showed
275 RSDs \leq 11 % ($n=4$) in tap water; suitable reproducibility was also observed in the surface water, obtaining
276 RSDs lower than 12 % ($n=3$).

277 Selectivity of detection was confirmed comparing the HPLC-FD profile of a “blank” river water SPE extract
278 and the one of the same river water sample spiked with 20 ng L⁻¹ of each FQ prior pre-concentration (Fig. 6).
279 Moreover, as FQs are detected as native compounds, information provided by fluorescence detection is
280 valuable in terms of selectivity [32,34,44].

281 Good linearity ($r^2 > 0.9991$) was found for the 5 drugs in the concentration range 1-50 µg L⁻¹, in agreement
282 with literature [39]. Regarding method sensitivity, MDL and MQL experimentally determined in raw river
283 water were respectively 3 ng L⁻¹ and 10 ng L⁻¹, except for CIP and DAN that were quantitatively determined
284 at concentrations ≥ 20 ng L⁻¹ (see Table 1). The sensitivity achieved is comparable with or better than that
285 reported for FQs in natural waters (see Table 2), thus g-C₃N₄@silica appears as a suitable sorbent for
286 determination at the low nanograms per litre.

287 Compared to silica derivatized with graphene [34] or pyrolyzed Kraft lignin [32], this preparation is easier
288 (one-pot, just need for ethanol and dicyandiamide); moreover, great advantage is gained in terms of costs in
289 comparison with graphene (dicyandiamide 0.025 €/g, graphene oxide 272.44 €/g, April 2016 prices).

290

291 **3.4 Application to real surface water samples**

292 g-C₃N₄@silica was applied to SPE of environmental samples, i.e. lake, river and ditch water, collected in the
293 Lombardy plain (Northern Italy). As it can be seen in Table 3, FQs were detected in all samples, attesting
294 their environmental diffusion in surface waters.

295 In particular, while in these lake and river water samples FQs amounts were below MDLs and/or MQLs, the
296 veterinary MAR and ENR were quantified at tens nanograms per litre in the ditch directly receiving swine
297 farms effluents, thus underlining the environmental impact of livestock farming.

298

299 **4. Conclusions**

300 Graphitic carbon nitride obtained from dicyandiamide has been supported onto silica microparticles,
301 characterized and tested for solid-phase extraction of FQ emerging contaminants from natural waters. g-
302 C₃N₄@silica was successfully employed for FQs determination in actual surface water samples prior HPLC-
303 FD, obtaining sensitivity better than or similar to that achieved using current carbon-based sorbents,
304 including graphene, but at remarkably lower costs. The material preparation is environmentally benign,

305 simple (one-pot), inexpensive and reproducible. g-C₃N₄@silica is efficient for enrichment of FQs from
306 aqueous complex matrices, and can be employed for more than one pre-concentration. The results here
307 presented contribute to enlarge the application of g-C₃N₄ for analytical purposes. It is believable that use of
308 supported g-C₃N₄ for column-extractions could be extended to other contaminants.

309

310 **Acknowledgments**

311 The Authors want to thank Dr. Gianluca A. Artioli for experimental support in material preparation.

312

313 **References**

314 [1] X. Zhang, X. Xie, H. Wang, J. Zhang, B. Pan, Y. Xie, Enhanced photoresponsive ultrathin graphitic-
315 phase C₃N₄ nanosheets for bioimaging, *J. Am. Chem. Soc.* 135 (2013) 18-21.

316 [2] X. Wang, K. Maeda, A. Thomas, K. Takanabe, G. Xin, J.M. Carlsson, A metal-free polymeric
317 photocatalyst for hydrogen production from water under visible light, *Nat. Mater.* 8 (2009) 76-80.

318 [3] P. Niu, L. Zhang, G. Liu, H. Cheng, Graphene-like carbon nitride nanosheets for improved photocatalytic
319 activities, *Adv. Funct. Mater.* 22 (2012) 4763-4770.

320 [4] N. Xu, Y. Wang, M. Rong, Z. Ye, Z. Deng, X. Chen, Facile preparation and applications of graphitic
321 carbon nitride coating in solid-phase microextraction, *J. Chromatogr. A* 1364 (2014) 53-58.

322 [5] J. Yang, L. Si, S. Cui, W. Bi, Synthesis of a graphitic carbon nitride nanocomposite with magnetite as a
323 sorbent for solid phase extraction of phenolic acids, *Microchim. Acta* 182 (2015) 737-744.

324 [6] M. Wang, H. Yuan, W. Deng, W. Bi, X. Yang, A Taiji-principle-designed magnetic porous C-doped
325 graphitic carbon nitride for environment-friendly solid phase extraction of pollutants from water samples, *J.*
326 *Chromatogr. A* 1412 (2015) 12-21.

327 [7] M. Wang, X. Yang, W. Bi, Application of magnetic graphitic carbon nitride nanocomposites for the
328 solid-phase extraction of phthalate esters in water samples, *J. Sep. Sci.* 38 (2015) 445-452.

329 [8] W. Guan, Z. Long, J. Liu, Y. Hua, Y. Ma, H. Zhang, Unique graphitic carbon nitride nanovessels as
330 recyclable adsorbent for solid phase extraction of benzoylurea pesticides in juices samples, *Food Anal.*
331 *Methods* 8 (2015) 2202-2210.

- 332 [9] H.B. Zheng, J.D. Ding, S.J. Zheng, G.T. Zhu, B.F. Yuan, Y.Q. Feng, Facile synthesis of magnetic carbon
333 nitride nanosheets and its application in magnetic solid phase extraction for polycyclic aromatic
334 hydrocarbons in edible oil samples, *Talanta* 148 (2016) 46-53.
- 335 [10] X. Fan, Y. Feng, Y. Su, L. Zhang, Y. Lv, A green solid-phase method for preparation of carbon nitride
336 quantum dots and their applications in chemiluminescent dopamine sensing, *RSC Adv.* 5 (2015) 55158-
337 55164.
- 338 [11] H. Li, F. Q. Shao, H. Huang, J.J. Feng, A.J. Wang, Eco-friendly and rapid microwave synthesis of green
339 fluorescent graphitic carbon nitride quantum dots for vitro bioimaging, *Sensor. Actuat. B: Chem.* 226 (2016)
340 506-511.
- 341 [12] Z. Mo, X. She, Y. Li, L. Liu, L. Huang, Z. Chen, Q. Zhang, H. Xu, H. Li, Synthesis of g-C₃N₄ at
342 different temperatures for superior visible/UV photocatalytic performance and photoelectrochemical sensing
343 of MB solution, *RSC Adv.* 5 (2015) 101552-101562.
- 344 [13] L. Malavasi et al., manuscript in preparation.
- 345 [14] A. Speltini, M. Sturini, F. Maraschi, A. Profumo, Recent trends in the application of the newest
346 carbonaceous materials for magnetic solid-phase extraction of environmental pollutants, *Trends Environ.*
347 *Anal. Chem.* 10 (2016) 11-23.
- 348 [15] Y.P. Sun, W. Ha, J. Chen, H.Y. Qi, Y.P. Shi, Advances and applications of graphitic carbon nitride as
349 sorbent in analytical chemistry for sample pretreatment: a review, *Trends Anal. Chem.* 2016, DOI:
350 10.1016/j.trac.2016.03.002.
- 351 [16] M. Rajabi, A.G. Moghadam, B. Barfi, A. Asghari, Air-assisted dispersive micro-solid phase extraction
352 of polycyclic aromatic hydrocarbons using a magnetic graphitic carbon nitride nanocomposite, *Microchim.*
353 *Acta.* 183 (2016) 1449-1458.
- 354 [17] X. Ding, J. Zhu, Y. Zhang, Q. Xia, W. Bi, X. Yang, J. Yang, Separation and concentration of natural
355 products by fast forced adsorption using well-dispersed velvet-like graphitic carbon nitride with response
356 surface methodology optimization, *Talanta* 154 (2016) 119-126.
- 357 [18] A. Speltini, M. Sturini, F. Maraschi, A. Profumo, A. Albini, Analytical methods for the determination of
358 fluoroquinolones in solid environmental matrices, *Trends Anal. Chem.* 30 (2011) 1337-1350.

359 [19] X. Van Doorslaer, J. Dewulf, H. Van Langenhove, K. Demeestere, Fluoroquinolone antibiotics: an
360 emerging class of environmental micropollutants, *Sci. Total Environ.* 500-501 (2014) 250-269.

361 [20] T. Reemtsma, M. Jekel, *Organic Pollutant in the Water Cycle*, Wiley-VCH, Weinheim, 2006.

362 [21] M. Lillenberg, S. Yurchenko, K. Kipper, K. Herodes, V. Pihl, K. Sepp, R. Löhmus, L. Nei,
363 Simultaneous determination of fluoroquinolones, sulfonamides and tetracyclines in sewage sludge by
364 pressurized liquid extraction and liquid chromatography electrospray ionization-mass spectrometry, *J.*
365 *Chromatogr. A.* 1216 (2009) 5949-5954.

366 [22] A. Speltini, M. Sturini, F. Maraschi, S. Viti, D. Sbarbada, A. Profumo, Fluoroquinolone residues in
367 compost by green enhanced microwave-assisted extraction followed by ultra performance liquid
368 chromatography tandem mass spectrometry, *J. Chromatogr. A.* 1410 (2015) 44-50.

369 [23] L. Ge, G. Na, S. Zhang, K. Li, P. Zhang, H. Ren, Z. Yao, New insights into the aquatic photochemistry
370 of fluoroquinolone antibiotics: direct photodegradation, hydroxyl-radical oxidation, and antibacterial activity
371 changes, *Sci. Total Environ.* 527-528 (2015) 12-17.

372 [24] M. Sturini, A. Speltini, F. Maraschi, L. Pretali, E. N. Ferri, A. Profumo, Sunlight-induced degradation of
373 fluoroquinolones in wastewater effluent: photoproducts identification and toxicity, *Chemosphere* 134 (2015)
374 313-318.

375 [25] A. Speltini, M. Sturini, F. Maraschi, A. Profumo, A. Albini, Microwave-assisted extraction and
376 determination of enrofloxacin and danofloxacin photo-transformation products in soil, *Anal. Bioanal. Chem.*
377 404 (2012) 1565-1569.

378 [26] S. Kusari, D. Prabhakaran, M. Lamshöft, M. Spiteller, In vitro residual anti-bacterial activity of
379 difloxacin, sarafloxacin and their photoproducts after photolysis in water, *Environ. Pollut.* 157 (2009) 2722-
380 2730.

381 [27] P. Sukul, M. Lamshöft, S. Kusari, S. Zühlke, M. Spiteller, Metabolism and excretion kinetics of ¹⁴C-
382 labeled and non-labeled difloxacin in pigs after oral administration, and antimicrobial activity of manure
383 containing difloxacin and its metabolites, *Environ. Res.* 109 (2009) 225-231.

384 [28] F. Tamtam, F. Mercier, J. Eurin, M. Chevreuil, B. Le Bot, Ultra performance liquid chromatography
385 tandem mass spectrometry performance evaluation for analysis of antibiotics in natural waters, *Anal.*
386 *Bioanal. Chem.* 393 (2009) 1709-1718.

387 [29] B. Chen, W. Wang, Y. Huang, Cigarette filters as adsorbents of solid-phase extraction for determination
388 of fluoroquinolone antibiotics in environmental water samples coupled with high-performance liquid
389 chromatography, *Talanta* 88 (2012) 237-243.

390 [30] F.J. Lara, M.D. Olmo-Iruela, A.M. García-Campañ, On-line anion exchange solid-phase extraction
391 coupled to liquid chromatography with fluorescence detection to determine quinolones in water and human
392 urine, *J. Chromatogr. A* 1310 (2013) 91-97.

393 [31] M. Gros, S. Rodríguez-Mozaz, D. Barceló, Rapid analysis of multiclass antibiotic residues and some of
394 their metabolites in hospital, urban wastewater and river water by ultra-high-performance liquid
395 chromatography coupled to quadrupole-linear ion trap tandem mass spectrometry, *J. Chromatogr. A* 1292
396 (2013) 173-188.

397 [32] A. Speltini, M. Sturini, F. Maraschi, E. Mandelli, D. Vadivel, D. Dondi, A. Profumo, Preparation of
398 silica-supported carbon by Kraft lignin pyrolysis, and its use in solid-phase extraction of fluoroquinolones
399 from environmental waters, *Microchim. Acta* 2016, DOI: 10.1007/s00604-016-1859-7.

400 [33] A. Speltini, M. Sturini, F. Maraschi, A. Profumo, Fluoroquinolone antibiotics in environmental waters:
401 sample preparation and determination, *J. Sep. Sci.* 33 (2010) 1115-1131.

402 [34] A. Speltini, M. Sturini, F. Maraschi, L. Consoli, A. Zeffiro, A. Profumo, Graphene-derivatized silica as
403 an efficient solid-phase extraction sorbent for pre-concentration of fluoroquinolones from water followed by
404 liquid-chromatography fluorescence detection, *J. Chromatogr. A* 1379 (2015) 9-15.

405 [35] P. Xiao, Y. Zhao, T. Wang, Y. Zhan, H. Wang, J. Li, A. Thomas, J. Zhu, Polymeric carbon
406 nitride/mesoporous silica composites as catalyst support for Au and Pt nanoparticles, *Chem. Eur. J.* 20
407 (2014) 2872-2878.

408 [36] N. Dorival-García, A. Zafra-Gómez, F.J. Camino-Sánchez, A. Navalón, J.L. Vilchez, Analysis of
409 quinolone antibiotic derivatives in sewage sludge samples by liquid chromatography–tandem mass
410 spectrometry: comparison of the efficiency of three extraction techniques, *Talanta* 106 (2013) 104.

411 [37] A. Speltini, M. Sturini, F. Maraschi, A. Porta. A. Profumo, Fast low-pressurized microwave-assisted
412 extraction of benzotriazole, benzothiazole and benzenesulfonamide compounds from soil samples, *Talanta*
413 147 (2016) 322-327.

414 [38] P. Vazquez-Roig, R. Segarra, C. Blasco, V. Andreu, Y. Picó, Determination of pharmaceuticals in soils
415 and sediments by pressurized liquid extraction and liquid chromatography tandem mass spectrometry, *J.*
416 *Chromatogr. A* 1217 (2010) 2471-2483.

417 [39] M. Sturini, A. Speltini, F. Maraschi, E. Rivagli, A. Profumo, Solvent-free microwave-assisted extraction
418 of fluoroquinolones from soil and liquid chromatography-fluorescence determination, *J. Chromatogr. A* 1217
419 (2010) 7316-7322.

420 [40] A.B. Jorge, D.J. Martin, M.T.S. Dhanoa, A.S. Rahman, N. Makwana, J. Tang, A. Sella, F. Corà, S.
421 Firth, J.A. Darr, P.D. McMillan, H₂ and O₂ evolution from water half-splitting reactions by graphitic carbon
422 nitride materials, *J. Phys. Chem. C* 117 (2013) 7178-7185.

423 [41] B. Jürgens, E. Irran, J. Senker, P. Kroll, H. Müller, W. Schnick, Melem (2,5,8-triamino-tri-s-triazine),
424 an important intermediate during condensation of melamine rings to graphitic carbon nitride: synthesis,
425 structure determination by X-ray powder diffractometry, solid-state NMR, and theoretical studies, *J. Am.*
426 *Chem. Soc.* 125 (2003) 10288-10300.

427 [42] M.L. Testa, M.L. Tummino, S. Agostini, P. Avetta, F. Deganello, E. Montoneri, G. Magnacca, A.
428 Bianco Prevot, Synthesis, characterization and environmental application of silica grafted photoactive
429 substances isolated from urban biowaste, *RSC Adv.* 5 (2015) 47920-47927.

430 [43] B. Zhu, P. Xia, W. Ho, J. Yu, Isoelectric point and adsorption activity of porous g-C₃N₄, *Appl. Surf. Sci.*
431 344 (2015) 188-195.

432 [44] M. Sturini, A. Speltini, L. Pretali, E. Fasani, A. Profumo, Solid-phase extraction and HPLC
433 determination of fluoroquinolones in surface waters. *J. Sep. Sci.* 32 (2009) 3020-3028.

434 [45] J.E. Renew, C.H. Huang, Simultaneous determination of fluoroquinolone, sulfonamide, and
435 trimethoprim antibiotics in wastewater using tandem solid phase extraction and liquid chromatography–
436 electrospray mass spectrometry, *J. Chromatogr. A* 1042 (2004) 113-121.

437 [46] M. Seifrtová, A. Pena, C.M. Lino, P. Solich, Determination of fluoroquinolone antibiotics in hospital
438 and municipal wastewaters in Coimbra by liquid chromatography with a monolithic column and fluorescence
439 detection, *Anal. Bioanal. Chem.* 391 (2008) 799-805.

440

441

442 **Figure captions**

443 **Fig. 1** XRD patterns (a) and TGA curves (b) for SiO₂, g-C₃N₄@silica 20 wt%, and g-C₃N₄.

444 **Fig. 2** SEM images at 10.000X and 25.000X for silica (a, b), and g-C₃N₄@silica 20 wt% (c, d).

445 **Fig. 3** FTIR spectra for SiO₂, g-C₃N₄@silica 20 wt%, and g-C₃N₄.

446 **Fig. 4** Effect of type eluting solution (a), sorbent amount (b) and eluting volume (c). Samples: 250 mL tap
447 water spiked with 100 ng L⁻¹ of each FQ (*n*=4).

448 **Fig. 5** HPLC-FD chromatogram obtained by SPE of tap water (500 mL) spiked with 20 ng L⁻¹ FQs.

449 **Fig. 6** HPLC-FD chromatograms overlay of raw river water (500 mL) SPE extract and the SPE extract of the
450 same river water sample spiked with 20 ng L⁻¹ of each FQ prior pre-concentration.

451

452 **Table titles**

453 **Table 1** Mean recoveries (%) and inter-day precision (RSD%) obtained by g-C₃N₄@silica SPE of tap and
454 river water samples spiked with each compound. Conditions: 100 mg sorbent, 6 mL 25 mM H₃PO₄ aqueous
455 solution-ACN (80:20) elution, sample volume 50-500 mL (native pH).

456 **Table 2** Comparison with recent analytical methods for SPE of FQs from natural waters.

457 **Table 3** FQs amounts determined in actual surface water samples by SPE on g-C₃N₄@silica followed by
458 HPLC-FD.

Figure 1

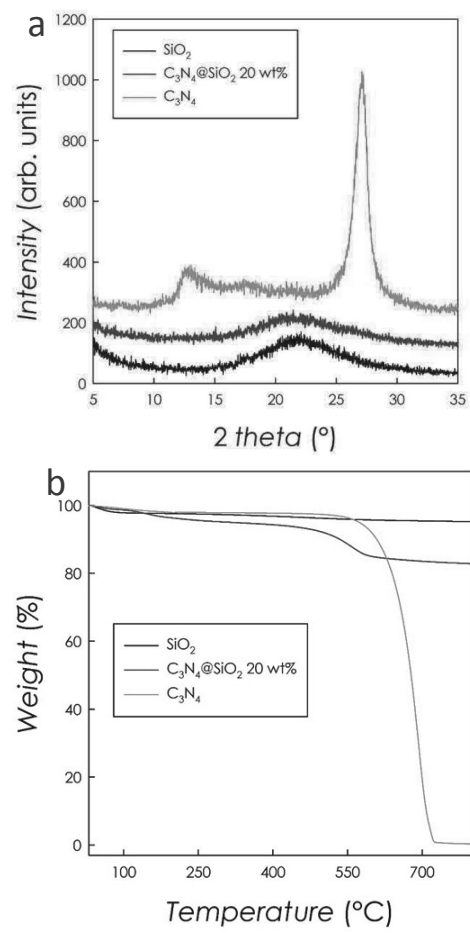


Figure 2

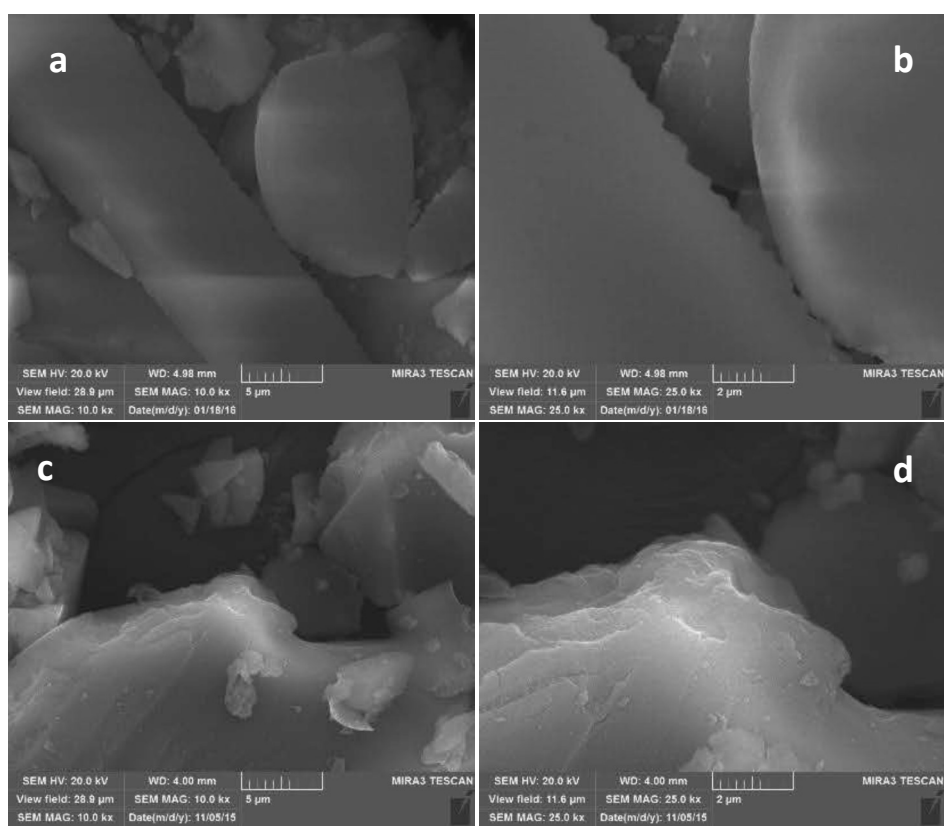


Figure 3

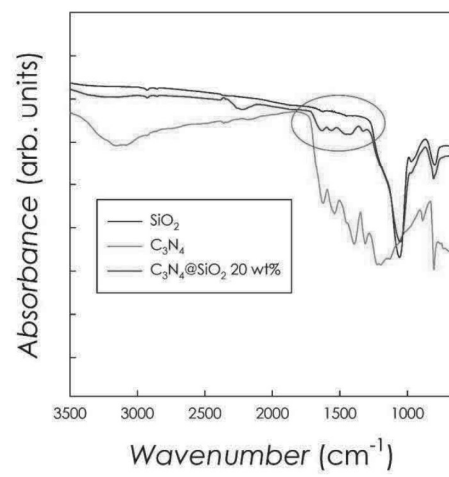


Figure 4

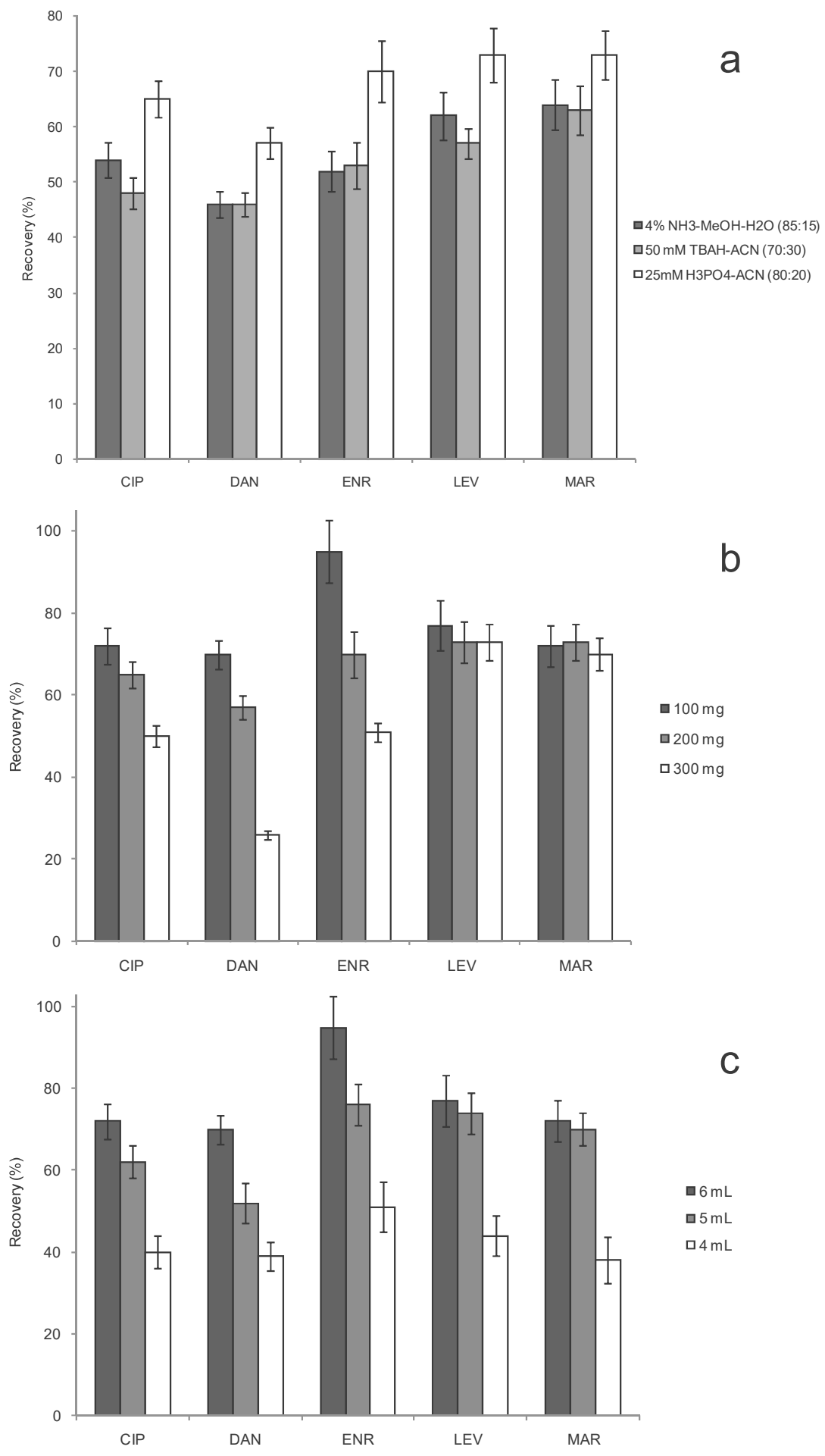


Figure 5

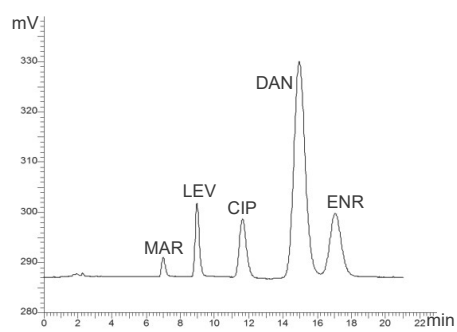


Figure 6

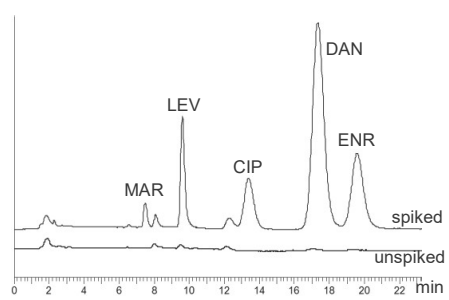


Table 1

Mean recovery (%) and inter-day precision ^a								
<i>Spike (ng L⁻¹)</i>	Tap water (<i>n</i> =4)				River water (<i>n</i> =3)			
	<i>100</i>	<i>50</i>	<i>20</i>	<i>10</i>	<i>100</i>	<i>50</i>	<i>20</i>	<i>10</i>
CIP	72 (6)	70 (6)	73 (8)	89 (8)	85 (8)	70 (8)	90 (10)	66 (12)
DAN	70 (5)	71 (7)	82 (11)	88 (9)	74 (8)	71 (9)	70 (11)	55 (14)
ENR	95 (8)	70 (5)	76 (8)	100 (11)	101 (9)	80 (9)	99 (10)	76 (12)
LEV	77 (8)	80 (7)	92 (10)	101 (9)	91 (9)	80 (9)	82 (10)	84 (11)
MAR	72 (7)	73 (8)	70 (9)	92 (10)	80 (9)	70 (9)	75 (10)	114 (12)

^a reported in parentheses as RSD%

Table 2

Sorbent material	MQL (ng L ⁻¹)	Determination	Ref.
HLB ^a	4-26	UHPLC-MS	28
HLB	1.81-45.17	UHPLC-MS	31
Cigarette filters	2-5	HPLC-UV	29
HyperSep Retain AX ^b	10-260	HPLC-FD	30
GN-silica ^c	5	HPLC-FD	34
LG-silica ^d	20	HPLC-FD	32
g-C ₃ N ₄ @silica	10-20	HPLC-FD	This work

^a hydrophilic-lipophilic balanced polymer

^b anion exchange polymer

^c silica-supported graphene

^d silica-supported pyrolyzed Kraft lignin

Table 3

Sample	FQs concentrations (ng L ⁻¹)				
	CIP	DAN	ENR	LEV	MAR
Adda River	n.d.	< 20	< 10	< 10	< 10
Naviglio Pavese River	< 20	< 20	< 10	< 10	< 10
Garda Lake	< 20	< 20	< 10	< 10	< 10
Farm ditch 1	n.d.	n.d.	31 ^a	n.d.	27 ^a

^a RSD < 12% (*n*=3)

n.d. not detected

Electronic Supplementary Material (online publication only)

[Click here to download Electronic Supplementary Material \(online publication only\): Supplementary Data.docx](#)